

## Electronic Supplementary Information (ESI)

### Room-Temperature Synthesis of a Fluorine-Functionalized Nanoporous Organic Polymer for Efficient SF<sub>6</sub> Separation

Jiangli Zhu,<sup>a†</sup> Danchi Luo,<sup>a†</sup> Qilin Wang,<sup>a</sup> Sihang Tong,<sup>a</sup> Zefeng Wang,<sup>b,c</sup> and Jun Yan,<sup>\*a</sup>

*<sup>a</sup>International Scientific and Technological Cooperation Base of Industrial Solid Waste Cyclic Utilization and Advanced Materials, School of Materials Science and Engineering, North Minzu University, Yinchuan 750021, China*

*<sup>b</sup>College of Ecology, Lishui University, Lishui 323000, China*

*<sup>c</sup>R&D Center of Green Manufacturing New Materials and Technology of Synthetic Leather Sichuan University-Lishui University, Lishui 323000, China*

Corresponding Authors:

Dr. Jun Yan; Email: yanjun2018@nun.edu.cn;

<sup>†</sup>J. Z. and D. L. contributed equally to this work.

# Contents

## Experimental Section

**Figure S1.** TGA curve (a) and wide-angle X-ray diffraction (b) of ANOP-8.

**Figure S2.** FE-SEM photo of ANOP-8.

**Figure S3.** (a) N<sub>2</sub> adsorption-desorption isotherms of ANOP-8 at 77 K; (b) Pore size distribution of ANOP-8 calculated by non-local density function (NLDFIT).

**Figure S4.** 77 K N<sub>2</sub> adsorption isotherms of ANOP-8 prepared in different batches.

**Figure S5.** FTIR spectrum of ANOP-8 after 7 d treatment in 1M HCl and 1M KOH.

**Figure S7.** Wide-angle X-ray diffraction (WAXD) of ANOP-8 after 7 d treatment in 1M HCl and 1M KOH.

**Figure S7.** N<sub>2</sub> adsorption-desorption isotherms of ANOP-8 after 7 d treatment in 1M HCl and 1M KOH at 77 K.

**Figure S8.** FTIR spectrum of ANOP-8 before and after SF<sub>6</sub> adsorption.

**Figure S9.** Wide-angle X-ray diffraction of ANOP-8 before and after SF<sub>6</sub> adsorption.

**Figure S10.** N<sub>2</sub> adsorption and desorption isotherms of ANOP-8 before and after SF<sub>6</sub> adsorption at 77 K

**Figure S11.** Adsorption isotherms and single-site Langmuir-Freundlich fitting curves for SF<sub>6</sub> and N<sub>2</sub> in ANOP-8 at 273 K and 298 K;

**Figure S12.** Isothermic heat of adsorption for SF<sub>6</sub> and N<sub>2</sub> of ANOP-8 polymer.

**Figure S13.** Optimized geometries of the ANOP-8 complexes (ANOP-8@SF<sub>6</sub> and ANOP-8@N<sub>2</sub>) calculated using Material Studio.

**Figure S14.** Scheme of the dynamic breakthrough apparatus.

**Table S1.** The chemical composition of ANOP-8 based on X-ray Photoelectron Spectroscop.

**Table S2.** Single-site Langmuir-Freundlich simulated parameters for ANOP-8.

**Table S3.** The virial equation fitted parameters for the isosteric heat of adsorption of ANOP-8 with SF<sub>6</sub> and N<sub>2</sub>

**Table S4.** Breakthrough time, adsorption uptake, diffusivity and selectivity of SF<sub>6</sub> and N<sub>2</sub> obtained from breakthrough experiments conducted at 298 K

## Experimental Section

### Materials

N,N,N',N'-tetraphenylbenzidine (97%), 2,3,4,5,6-pentafluorobenzaldehyde, trifluoromethanesulfonic acid, potassium hydroxide (85%) anhydrous dimethylsulfoxide (DMSO), anhydrous N, N-dimethylformamide (DMF), dichloromethane (DCM), anhydrous tetrahydrofuran (THF) were provided by J&K Chemical Co., Ltd.

### Synthesis of ANOP-8

Under a nitrogen atmosphere, N,N,N',N'-tetraphenylbenzidine (0.73 g, 1.5 mmol), 2,3,4,5,6-pentafluorobenzaldehyde (0.59 g, 3.0 mmol), and CH<sub>2</sub>Cl<sub>2</sub> (20.0 mL) were added to a dry Schlenk flask equipped with a stirrer and a dropping funnel. The mixture was stirred at room temperature for 30 min. Subsequently, trifluoromethanesulfonic acid (1.5 mL, 18 mmol) was added dropwise over a period of 20 min, and the reaction mixture was stirred for 12 h. Upon completion of the reaction, the resulting solid was isolated by filtration and sequentially washed with 1 M NaOH aqueous solution, distilled water, DMSO, DMF, and THF. The product was then subjected to Soxhlet extraction with THF for 48 h and finally dried under vacuum at 130 °C for 24 h. Yield: 81%.

### Material Characterization

The morphology of the as-prepared polymers was examined by field-emission scanning electron microscopy (FE-SEM) conducted using a SUPRA™ 55 microscope (ZEISS). X-ray diffraction (XRD) was performed on a Rigaku D Max 2400 X-ray diffractometer (40 kV, 200 mA) with a copper target and a scanning rate of 2°/min. Thermogravimetric analysis (TGA) was conducted using a Q50 thermogravimetric analyzer (TA Instruments) under sample heating from room temperature to 800 °C in a nitrogen (N<sub>2</sub>) atmosphere at a rate of 10°C/min rate. The chemical structure of the as-prepared polymers was evaluated by Fourier transform infrared (FTIR) spectroscopy using a Nicolet™ 20XB spectrophotometer (ThermoFisher Scientific). Solid-state <sup>13</sup>C cross-polarization/total suppression of spinning sidebands (CP/TOSS) NMR spectra were recorded

on a Bruker AVANCE III HD 600 MHz Ascend wide-bore spectrometer. X-ray photoelectron spectroscopy (XPS) measurements were carried out using a Thermo Scientific K-Alpha instrument, manufactured by Thermo Fisher Scientific, USA. The spectrometer was operated with an aluminum  $K\alpha$  X-ray source, characterized by a photon energy of 1486.6 eV. Binding energy calibration was performed using the C1s peak at 284.80 eV as a reference to ensure accuracy in the binding energy measurements. The  $N_2$  sorption isotherms (77 K) of the as-synthesized polymers were analyzed using a Quantachrome Instruments Autosorb iQ gas sorption analyzer. Adsorption measurements for  $N_2$  and  $SF_6$  were performed using a gas adsorption analyzer (BSD-PMC, BeiShiDe Instrument Co. Ltd., China). The calculated adsorption selectivities of  $SF_6/N_2$  is based on the ideal adsorbed solution theory (IAST), which involved fitting single-site Langmuir-Freundlich curves to the single-component  $SF_6$  and  $N_2$  adsorption isotherms collected at 273 and 298 K. The  $SF_6/N_2$  gas compositions were set as 0.1/0.9. Dynamic gas breakthrough experiments were performed using a quartz column (0.6 cm ID  $\times$  7.5 cm) filled with 0.20 g of ANOP-8. Prior to the breakthrough tests, the sample was activated by a helium flow of 40 mL $\cdot$ min $^{-1}$  at 373 K for 3 h. A gas mixture containing  $SF_6$  and  $N_2$  in the concentrations of 10% and 90% respectively (v/v) was introduced at a constant flow rate of 20 mL $\cdot$ min $^{-1}$  at 298 K. Gas composition was analyzed using a ThermoStar system (Pfeiffer Vacuum, Inc.), based on ion peaks detected at m/z values of 64 for  $SF_6$  and 28 for  $N_2$ . By recording the breakthrough curves (the outlet concentration as a function of time), we determined the adsorption capacity of the adsorbent.

### **Computational details**

To gain further insight to interaction of  $SF_6$  and  $N_2$  with ANOP-8, we carried out theoretical calculations using density-functional theory (DFT) and Forcite modules of Material Studio.

### **Estimation of the Isosteric heats of $SF_6$ and $N_2$ gas adsorption**

The virial method was employed to calculate the enthalpies of adsorption for  $SF_6$  and  $N_2$  (273 and 298 K) on ANOP-8 polymer.<sup>1</sup> In each case, the data were fitted using the equation:

$$\ln(P) = \ln(N) + 1/T \sum_{i=0}^m a_i N^i + \sum_{i=0}^m b_i N^i \quad \text{S1}$$

Here,  $P$  is the pressure expressed in mmHg,  $N$  is the quantity adsorbed in mg/g,  $T$  is the temperature in K,  $a_i$  and  $b_i$  are virial coefficients,  $m$  and  $n$  represent the number of coefficients required to adequately describe the isotherms ( $m$  and  $n$  were gradually increased until the contribution of extra added  $a$  and  $b$  coefficients was deemed to be statistically insignificant towards the overall fit, and the average value of the squared deviations from the experimental values was minimized). The values of the virial coefficients  $a_0$  through  $a_m$  were then used to calculate the isosteric heat of adsorption using the following expression

$$Q_{st} = -R \sum_{i=0}^m a_i N^i \quad \text{S2}$$

Where  $R$  is the universal gas constant ( $8.314 \text{ J K}^{-1} \text{ mol}^{-1}$ )  $Q_{st}$  is the coverage-dependent isosteric heat of adsorption and  $R$  is the universal gas constant.

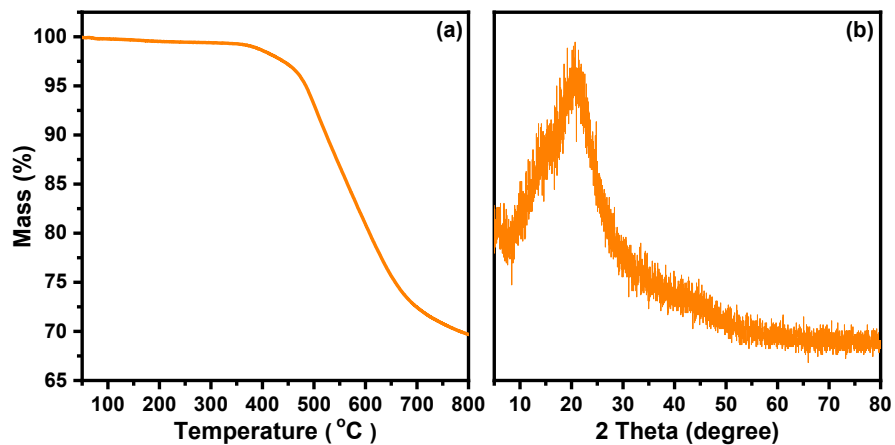


**Figure S1.** TGA curve (a) and wide-angle X-ray diffraction (b) of ANOP-8

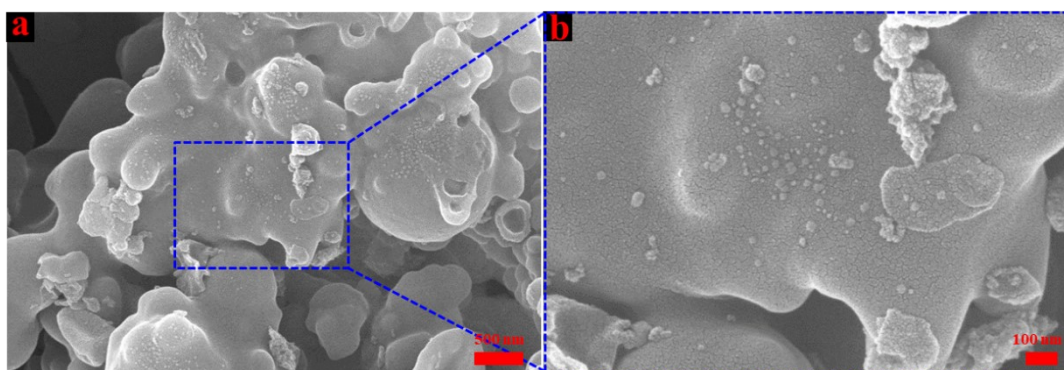


**Figure S2.** FE-SEM photo of ANOP-8.

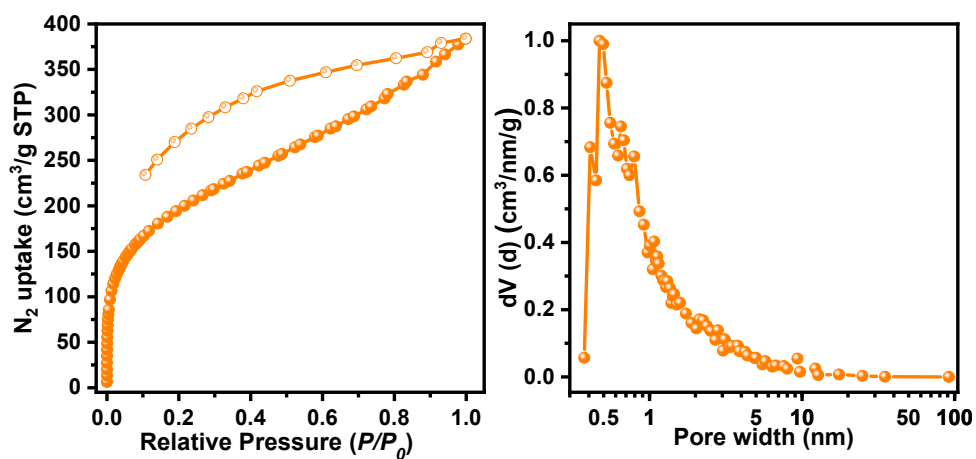


**Figure S3.** (a)  $N_2$  adsorption-desorption isotherms of ANOP-8 at 77 K; (b) Pore size distribution of ANOP-8 calculated by non-local density function (NLDFT).

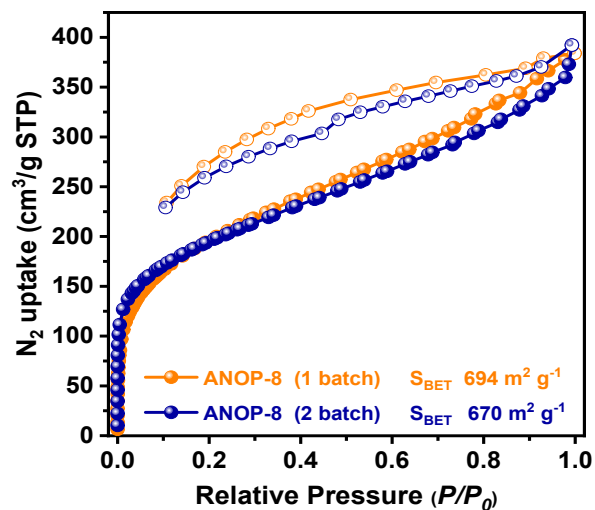


**Figure S4.** 77 K N<sub>2</sub> adsorption isotherms of ANOP-8 prepared in different batches.

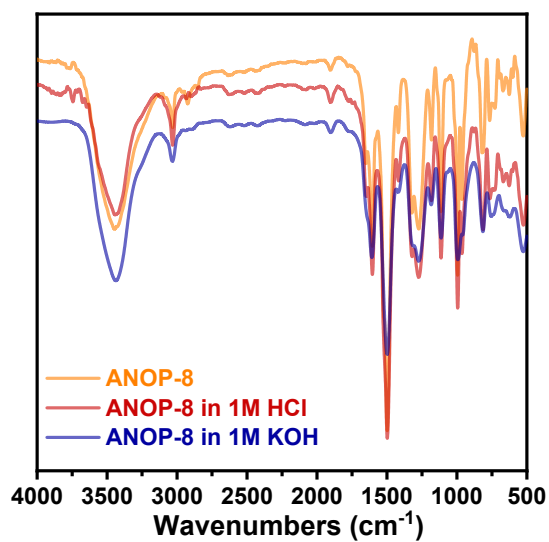


**Figure S5.** FTIR spectrum of ANOP-8 after 7 d treatment in 1M HCl and 1M KOH.



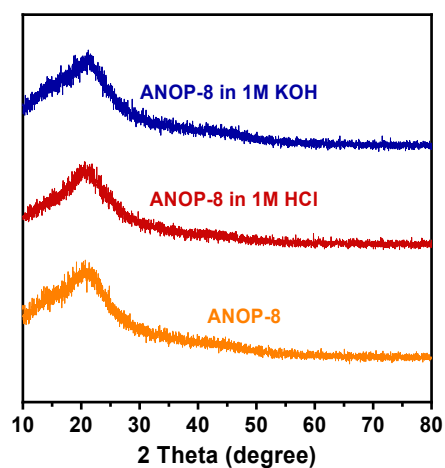


**Figure S6.** Wide-angle X-ray diffraction (WAXD) of ANOP-8 after 7 d treatment in 1M HCl and 1M KOH.

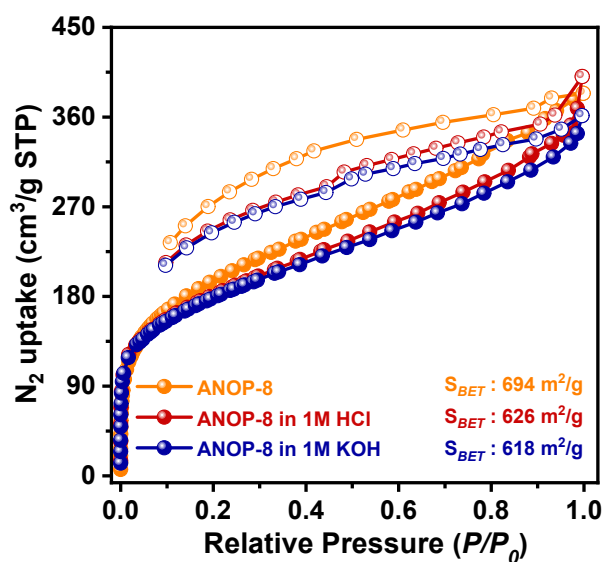


**Figure S7.**  $N_2$  adsorption-desorption isotherms of ANOP-8 after 7 d treatment in 1M HCl and 1M KOH at 77 K.

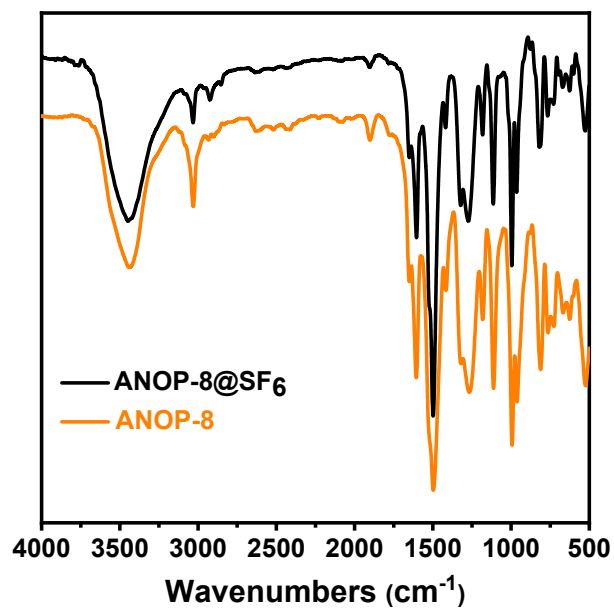


**Figure S8.** FTIR spectrum of ANOP-8 before and after SF<sub>6</sub> adsorption.

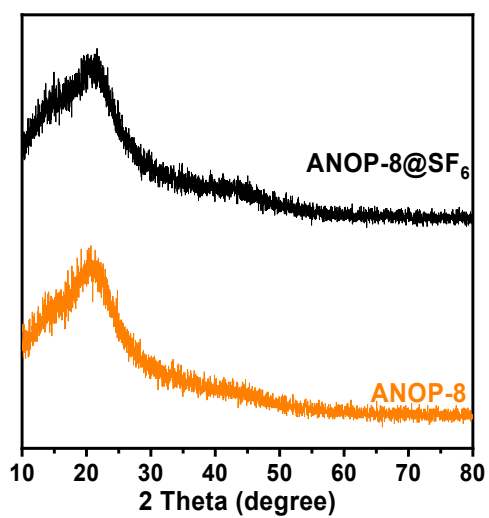


**Figure S9.** Wide-angle X-ray diffraction (WAXD) of ANOP-8 before and after SF<sub>6</sub> adsorption.

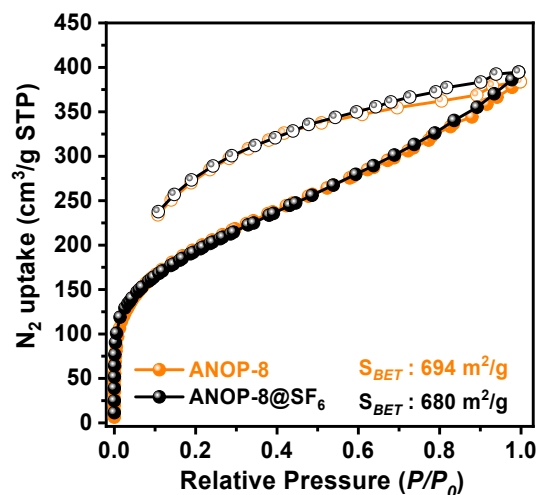


**Figure S10.**  $N_2$  adsorption and desorption isotherms of ANOP-8 before and after  $SF_6$  adsorption at 77 K.

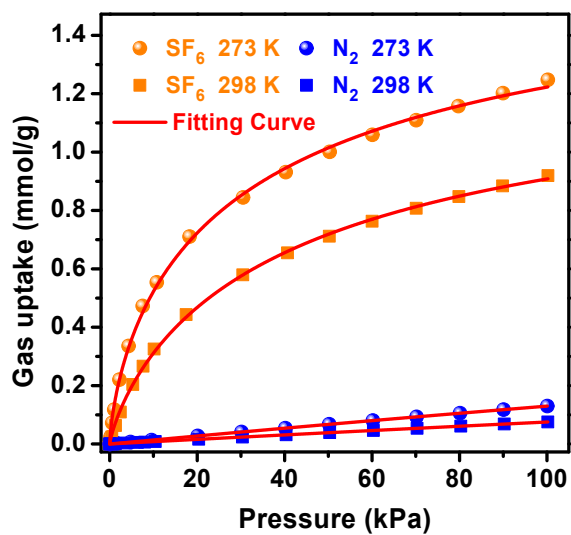


**Figure S11.** Adsorption isotherms and single-site Langmuir-Freundlich fitting curves for  $SF_6$  and  $N_2$  in ANOP-8 at 273 K and 298 K.

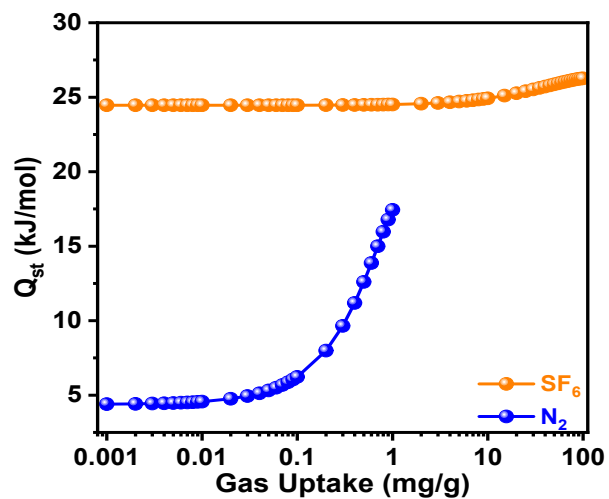


**Figure S12.** Isosteric heat of adsorption for SF<sub>6</sub> and N<sub>2</sub> of ANOP-8 polymer.

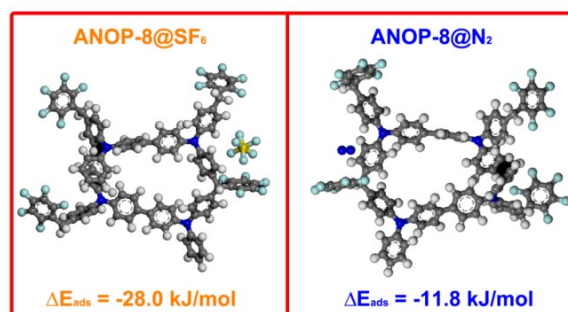


**Figure S13.** Optimized geometries of the ANOP-8 complexes (ANOP-8@SF<sub>6</sub> and ANOP-8@N<sub>2</sub>) calculated using Material Studio.

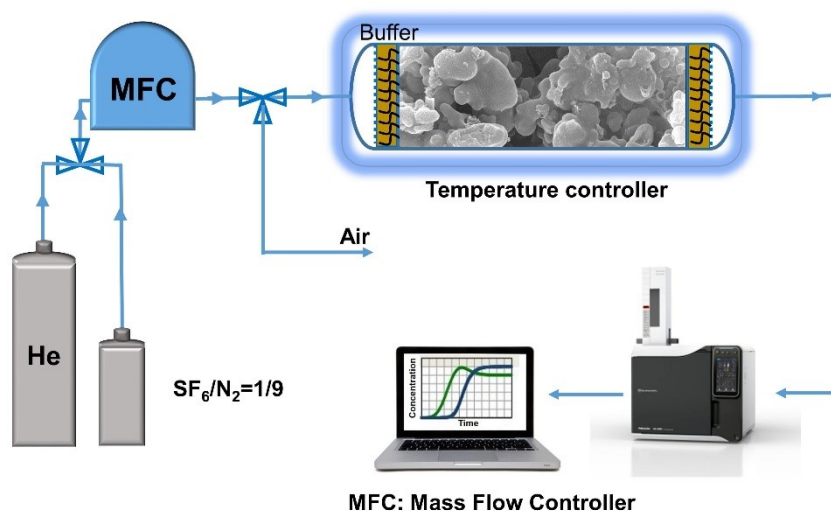


**Figure S14.** Scheme of the dynamic breakthrough apparatus.

The adsorption amount of adsorbent n is calculated according to the equation S3 as:

$$Q_{\text{nad}} = Q_{\text{nin}} - Q_{\text{nout}} = q_{\text{in}} \times C_{n0} \times \Delta T - \int_0^t [q/(1 - \sum_1^N C_{nt})] * C_{nt} dt \quad \text{S3}$$

$Q_{\text{nad}}$  is the adsorption amount of adsorbent n;  $Q_{\text{nin}}$  is the total flow rate of adsorbent n flowing in of the penetrating column at  $\Delta T$ ;  $Q_{\text{nout}}$  is the total flow rate of adsorbent n flowing out of the penetrating column at  $\Delta T$ ;  $q_{\text{in}}$  is the total flow rate of gas through the column inlet;  $C_{n0}$  is the total flow rate of gas through the outlet of the column;  $\Delta T$  is the total adsorption time (min);  $q$  is the flow rate of carrier gas;  $C_{nt}$  is the percentage concentration of adsorbent N at the entrance of the penetrating column;

The selectivity of gas (1) over gas (2) is calculated according to the equation S4 as:

$$S = \left(\frac{X_1}{Y_1}\right) \div \left(\frac{X_2}{Y_2}\right) \quad \text{S4}$$

$X_1/Y_1$ : Molar fraction of component 1 in the adsorbed phase/molar fraction of component 1 in the gas phase.

$X_2/Y_2$ : Molar fraction of component 2 in the adsorbed phase/molar fraction of component 2 in the gas phase.

The diffusion coefficient of gas

$$D = \frac{L^2}{6t_{\text{eq}}} \quad \text{S5}$$

D is the diffusion coefficient of vapor; L is the loading length;  $t_{\text{eq}}$  is the delay time.

**Table S1.** The chemical composition of ANOP-8 based on X-ray photoelectron spectroscopy.

Sample	Element	Experimental (wt%)	Theoretical (wt%)
ANOP-8	C	82.49	71.09
	F	14.86	22.51
	N	2.65	3.32
	H	-	3.08

**Table S2.** Single-site Langmuir-Freundlich simulated parameters for ANOP-8

Sample	T/K	Gas	A1(mmol/g)	B1(kPa <sup>-C1</sup> )	C1	R <sup>2</sup>
ANOP-8	273 K	SF <sub>6</sub>	1.7985	7.8916×10 <sup>-2</sup>	0.7150	0.9991
		N <sub>2</sub>	1.4933	8.9882×10 <sup>-4</sup>	1.0120	0.9999
	298 K	SF <sub>6</sub>	1.3955	4.4263×10 <sup>-2</sup>	0.8121	0.9996
		N <sub>2</sub>	1.0411	7.4038×10 <sup>-4</sup>	1.0107	0.9999

**Table S3.** The virial equation fitted parameters for the isosteric heat of adsorption of ANOP-8 with SF<sub>6</sub> and N<sub>2</sub>

Samples	SF <sub>6</sub>	N <sub>2</sub>
a <sub>0</sub>	-2.9418×10 <sup>-3</sup>	-5.2676×10 <sup>2</sup>
a <sub>1</sub>	-6.5484	-2.2700×10 <sup>3</sup>
a <sub>2</sub>	0.10212	4.1838×10 <sup>2</sup>
a <sub>3</sub>	-1.0371×10 <sup>-3</sup>	3.8880×10 <sup>2</sup>
a <sub>4</sub>	5.7427×10 <sup>-6</sup>	-1.2073×10 <sup>2</sup>
a <sub>5</sub>	-1.2128×10 <sup>-8</sup>	13.002
b <sub>0</sub>	9.9186	7.2715
b <sub>1</sub>	2.2680×10 <sup>-2</sup>	8.9799
b <sub>2</sub>	-3.6103×10 <sup>-5</sup>	-3.3358
r <sup>2</sup>	0.9996	0.9962

**Table S4.** Breakthrough time, adsorption uptake, diffusivity and selectivity of SF<sub>6</sub> and N<sub>2</sub> obtained from breakthrough experiments conducted at 298 K

Samples	Gas	Breakthrough time (s/g)	Adsorption Uptake(cm <sup>3</sup> /g)	Diffusivity (cm <sup>2</sup> /s)	Selectivity (SF <sub>6</sub> /N <sub>2</sub> )
ANOP-8	SF <sub>6</sub>	150.3	7.51	0.130	51.1
	N <sub>2</sub>	8.4	1.32	1.530	

## Reference

1. W. Lu, D. Yuan, D. Zhao, C. I. Schilling, O. Plietzsch, T. Muller, S. Braese, J. Guenther, J. Blumel, R. Krishna, Z. Li and H.-C. Zhou, *Chem. Mater.*, 2010, **22**, 5964-5972.